



Atmospheric phase distribution of oxidized and reduced nitrogen at a forest ecosystem research site

Andreas Held^{a,*}, Thomas Wrzesinsky^a, Alexander Mangold^a, Jörg Gerchau^b,
Otto Klemm^a

^a Bayreuth Institute for Terrestrial Ecosystem Research, University of Bayreuth, BITÖK-Klimatologie, D-95440 Bayreuth, Germany

^b Institut für Stratosphärische Chemie (ICG-I), Forschungszentrum Jülich, D-52425 Jülich, Germany

Received 27 July 2001; received in revised form 15 February 2002; accepted 8 March 2002

Abstract

Atmospheric concentrations of gaseous NH_3 and HNO_3 and of particulate NH_4^+ and NO_3^- were measured during various seasons at a forest ecosystem research site in the “Fichtelgebirge” mountains in Central Europe. Air masses arriving at this site were highly variable with respect to trace compound concentration levels and their concentration ratios. However, the distributions of NH_4^+ and NO_3^- within the aerosol particle size spectra exhibited some very consistent patterns, with the former dominating the fine particle concentrations, and the latter dominating the coarse particles range, respectively. Overall, the particulate phase ($\text{NH}_4^+ + \text{NO}_3^-$) dominated the atmospheric nitrogen budget (particulate and gas phase, $\text{NH}_4^+ + \text{NO}_3^- + \text{NH}_3 + \text{HNO}_3$) by more than 90% of the median total mixing ratio in winter, and by more than 60% in summer. The phase partitioning varied significantly between the winter and summer seasons, with higher relative importance of the gaseous species during summer, when air temperatures were higher and relative humidities lower as compared to the winter season. Reduced nitrogen dominated over oxidized nitrogen, indicating the prevailing influence of emissions from agricultural activity as compared to traffic emissions at this mountainous site. A model has been successfully applied in order to test the hypothesis of thermodynamic equilibrium between the particulate and gas phases.

© 2002 Elsevier Science Ltd. All rights reserved.

Keywords: Atmospheric chemistry; Phase partitioning; Nitrogen species; Thermodynamic equilibrium

1. Introduction

Oxidized and reduced atmospheric nitrogen plays a crucial role in various biogeochemical processes such as the nutritional balance of terrestrial ecosystems (Matzner et al., 2001), and acid deposition (Schulze et al., 1989). The atmosphere acts as the major source of nitrogen input into ecosystems by three main pathways: (1) dry deposition of gases and particles, not associated

with precipitation water, (2) wet deposition of substances with precipitation, and (3) occult deposition, which is the deposition of fog droplets on vegetation due to gravitational settling and turbulent transport. Depending on their state of aggregation, their water solubility, as well as depending on the amount of available precipitation, and the physical and chemical characteristics of the receiving surfaces, various atmospheric trace substances are preferentially deposited through dry or wet deposition, respectively (Seinfeld and Pandis, 1998).

Fig. 1 gives a schematic overview of processes involved in the gas/particle partitioning and deposition of atmospheric nitrogen species. The main sources of atmospheric ammonia are agricultural emissions from domestic animal excreta and fertilizer usage. Nitric acid

* Corresponding author. Tel.: +49-921-55-5622; fax: +49-921-55-5799.

E-mail address: andreas.held@bitoek.uni-bayreuth.de (A. Held).

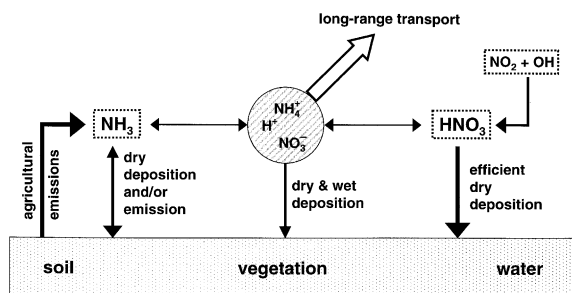


Fig. 1. Schematics of the processes and pathways that lead to reduced (NH_3 and NH_4^+) and oxidized (HNO_3 and NO_3^-) nitrogen in the atmospheric boundary layer. The circle in the center represents an (solid or liquid) aerosol particle, gases are drawn as dotted boxes, arrows represent fluxes, and double-arrows show bidirectional fluxes that tend to establish thermodynamic equilibrium.

is produced in the atmosphere through oxidation of NO_x , primarily by OH radicals. To a large extent, the particulate species of oxidized and reduced nitrogen are formed by gas-to-particle conversion reactions, such as the reaction of NH_3 and HNO_3 leading to ammonium nitrate. Thus, both NO_3^- and NH_4^+ are primarily secondary compounds of atmospheric particles (i.e., they are not directly emitted into, but are formed within the atmosphere). During fog episodes, the transfer of gaseous species to the aqueous phase is enhanced for substances with higher water solubilities, such as NH_3 and HNO_3 . This may lead to elevated amounts of particulate species during and after fog events as compared to dry weather conditions. The deposition mechanisms of gaseous and particulate compounds are quite different from each other. Particles may be removed from the atmosphere as wet deposition through rainout, washout or nucleation scavenging processes. Moreover, particles may be removed from the atmosphere by dry deposition, with particle size being the most important single factor determining the deposition velocity (e.g. Friedlander, 2000). Particles in the size range from 0.1 to 1.0 μm aerodynamic particle diameter exhibit the longest atmospheric residence times. Therefore, they are called "accumulation range" particles. Smaller particles act similar to gas molecules, which leads to effective deposition by Brownian diffusion, while deposition of larger particles is enhanced by gravitational settling. Accumulation range particles, however, are capable of travelling long distances through advective atmospheric transport before deposition.

In contrast, the deposition of gases is governed by their solubility, their reactivity, as well as the properties of the deposition surface. Nitric acid is highly water soluble, reacts readily with many gases and particles, and may be adsorbed on most surfaces. Therefore, HNO_3 is removed from the atmosphere very effectively

by both incorporation into wet particles and dry deposition. The latter process is limited primarily by atmospheric turbulence. The deposition processes for particulate nitrate (NO_3^-) are considerably slower, though being strongly dependent on particle size as mentioned above. The quantification of NH_3 deposition is complicated by the fact that, under certain circumstances, NH_3 may be emitted by vegetation or from soil surfaces. The possible emission of NH_3 is explained by the existence of a so-called compensation point concentration of NH_3 in the atmosphere (Sutton et al., 1995). At this concentration, an equilibrium between the atmospheric NH_3 concentration and the substomatal intercellular NH_4^+ concentration of the vegetation is established. For atmospheric NH_3 concentrations below the compensation point, ammonia is emitted from the canopy or soil surface. The compensation point itself is not a constant concentration but rather depends on various parameters such as air temperature, humidity, the type and nutritional state of the vegetation, and further factors. In general, ammonia is deposited rather briefly after emission near its source, whereas particulate ammonium (NH_4^+) may be carried thousands of kilometers through atmospheric long-range transport.

The distribution of $\text{NH}_3/\text{NH}_4^+$ and $\text{HNO}_3/\text{NO}_3^-$ in the gas and particulate phases affects the chemical reactivity of the atmosphere in various ways. NH_3 is the most important alkaline substance in the atmosphere (e.g. Seinfeld and Pandis, 1998) and of great relevance in all three phases for the neutralization of atmospheric acids such as HNO_3 or H_2SO_4 . HNO_3 may react with many gases and particles, thereby contributing to secondary particle formation and enrichment of nitrate in already existing aerosol particles. As HNO_3 is removed very effectively from the atmosphere, the formation of HNO_3 is a major sink for reactive atmospheric nitrogen compounds.

The above considerations reveal the importance of the phase distribution of oxidized and reduced nitrogen in the atmosphere. Its knowledge is a crucial prerequisite for a reliable quantification of deposition fluxes to determine atmospheric nitrogen input into ecosystems. For our site in the "Fichtelgebirge" mountains in North-eastern Bavaria, Matzner et al. (2001) applied the canopy balance method and arrived at estimates of the lower limit of nitrogen deposition of $1.5 \text{ kmol ha}^{-1} \text{ yr}^{-1}$ ($21 \text{ kg N ha}^{-1} \text{ yr}^{-1}$). For estimating the total deposition flux, however, canopy uptake of nitrogen must be taken into account as well. This contribution is largely unknown and may be as high as $2 \text{ kmol ha}^{-1} \text{ yr}^{-1}$.

In this paper, we report results from measurements of reduced ($\text{NH}_3/\text{NH}_4^+$) and oxidized ($\text{HNO}_3/\text{NO}_3^-$) nitrogen species in the gas and particulate phases conducted at our ecosystem research site during various seasons throughout the year. The atmospheric phase distribution of these species is studied with regard to microme-

teorological parameters, and finally, a thermodynamic model is applied to calculate the theoretical phase distribution of oxidized and reduced nitrogen according to a possible thermodynamic equilibrium. We consider these studies as an important step towards a better understanding of nitrogen cycling in terrestrial ecosystems.

2. Site and methods

Since 1990, the Bayreuth Institute for Terrestrial Ecosystem Research (BITÖK) has been studying forest ecosystems in the “Fichtelgebirge” mountain range in Northeastern Bavaria, Germany. Our measuring site “Waldstein/Pflanzgarten” is situated in a 100 m × 200 m forest clearing at 765 m a.s.l. (50° 08' 40" N, 11° 51' 55" E), surrounded by a forest with Norway spruce (*Picea abies* (L.) Karst.) as the dominant tree species. Especially in summer, westerly winds are prevailing, advecting marine air masses over Western and Central Europe to our site. In wintertime, however, easterly wind conditions occur more frequently and with longer duration, advecting dry continental air masses from Eastern Europe. Air quality measurements indicate that our site is a rural site in Central Europe (Klemm and Lange, 1999). It is situated quite remotely from large direct emission sources. The Halle-Leipzig industrial area is about 140 km to the North, and the lignite-fired power plants of Northern Bohemia are about 50 km to the East. A few, small farms exist nearby.

For size-resolved particle collection, a five-stage Berner low-pressure impactor (LPI80/0.05/2.88) with polyvinyl fluoride (Tedlar, DuPont) impaction surfaces was used. Table 1 lists the characteristics of our impactor.

The air flow rate is restricted to 75.4 l min⁻¹ (STP) through a critical orifice. From 1998 through 2000, a total of 86 sample sets was taken. Sampling intervals normally lasted from approximately 10 a.m. to 4 p.m. (CET), for a total of 6 h. These sampling intervals were selected as the best approximation to stationary atmospheric conditions, which is crucial for the investigation

of a possible thermodynamic equilibrium between the gas and particulate phases. In addition, 22 measurements were performed overnight and under variable meteorological conditions. Each impaction surface was extracted by shaking in double-demineralized water for 24 h overnight. After extraction, the samples were analyzed for ammonium by flow injection analysis, and for nitrate and sulfate by ion chromatography, respectively. To ensure high-quality chemical analysis, these measurements were performed by the certified BITÖK analytical laboratory. The reduced pressure conditions of the Berner impactor may lead to evaporation of semi-volatile ammonium nitrate and ammonium chloride. Therefore, the presented concentrations of particulate ammonium and nitrate should be taken as lower-limit values. However, we do not expect our measurements to be severely affected by the evaporation of ammonium nitrate. Blank samples were obtained briefly before each sampling interval and for each impactor stage by inserting impaction surfaces and starting the sampling process for a few seconds. Directly afterwards, the substrates were removed from the impactor and the 6 h sampling was prepared and started. The blank samples were analyzed analogously to all other samples. Because of the 6 h sampling intervals, and due to the selected analytical methods, the sample concentrations of the ions Na⁺, Ca²⁺, Mg²⁺, K⁺, and Cl⁻, were below their respective detection limits. However, previous studies in the “Fichtelgebirge” mountains revealed that NO₃⁻, SO₄²⁻, and NH₄⁺ dominate the ion balance in the atmospheric aerosol at our site (Ludwig and Klemm, 1990; Peters and Bruckner-Schatt, 1995). In addition, Wrzesinsky and Klemm (2000) showed that these three ions represent about 85% of the total ion charge in fog. Therefore, the error arising from the exclusion of all ions other than NO₃⁻, SO₄²⁻, and NH₄⁺ from further considerations is regarded to be minor.

We used the LAS-X laser particle spectrometer (PMS, Boulder, CO, USA) for the measurement of particle number concentrations. The optical particle counter detects and sizes aerosol particles through light scattering and the evaluation of the scattering intensity in 15 size bins ranging from 0.1 to 3 μm particle diameter. This covers most of the size range sampled with the Berner impactor.

Atmospheric concentrations of ammonia (NH₃) were determined by employing a horizontal continuous-flow wet denuder (AMANDA). For a detailed description of the sampling system see Wyers et al. (1993). Ambient air was sampled with a flow rate of 26.5 l min⁻¹ through a rotating annular ring covered by a thin film of 3.6 mM sodium hydrogen sulfate (NaHSO₄). The stripping solution containing NH₄⁺ was continuously sampled and replaced. After adding 0.5 M NaOH, molecular NH₃ was formed in the stripping solution which selectively passed a PTFE membrane, and was taken up as NH₄⁺

Table 1
Characteristics of the Berner impactor LPI80/0.05/2.88: 50% cut-off diameter and geometric mean diameter of the five sampling stages

Stage	50% cut-off diameter (μm)	Geometric mean diameter (μm)
	10	
5	3.5	5.9
4	1.2	2
3	0.42	0.71
2	0.14	0.25
1	0.05	0.085

in deionized water on the other side of the membrane. Then, NH_4^+ concentrations were determined by conductivity measurements. Ammonia is measured continuously at the “Waldstein” site since July 1997 with averaging intervals of 10 min. The system is calibrated every week. The 10 min-samples were averaged over the period of the impactor sampling intervals for comparison. Some short interruptions due to adverse weather conditions and servicing caused minor data losses.

Nitric acid (HNO_3) was measured using a modified wet annular denuder system after Keuken et al. (1988). In February, the measurement set up was periodically heated to prevent icing. Through teflon tubing, ambient air was pumped into the system, and through a rotating annular ring with an air flow rate of 32 l min^{-1} . Both walls of the ring were covered by double-demineralized water used as stripping solution. After 52.75 min of sampling, the stripping solution was pumped into an auto-sampler container. Then, the denuder was refilled and a new sampling cycle was started for a total sampling resolution of 1 h. The samples were collected each day and analyzed for nitrate by ion chromatography. On several occasions, the stripping solution was sampled without air flowing through the denuder. These measurements were taken as an estimation of blank samples and subtracted from all measurements. The HNO_3 denuder was employed during two intensive sampling periods in February and May of 2000, which represented typical wintertime and summertime conditions, respectively. The 1 h-resolved data were averaged over the sampling intervals of the impactor for the comparisons in this study.

For a theoretical estimation of the distribution of chemical species between the gas and particulate phases, a thermodynamic equilibrium model was used. We employed the Aerosol Inorganics Model AIM2 (Clegg et al., 1998) to study possible thermodynamic equilibria of reduced and oxidized nitrogen between the gas and the particulate phases, respectively. The input parameters for these calculations are air temperature, relative humidity, and the molar concentrations of H^+ , NH_4^+ , SO_4^{2-} , and NO_3^- ions to be distributed between the gas and particle phases. We calculated the initial NH_4^+ and NO_3^- concentrations from our impactor and denuder measurements as the sums of the gaseous and particulate species, respectively. For SO_4^{2-} , we only used the particulate fraction, and finally, we calculated H^+ to balance anion and cation concentrations, which is mandatory to run the model. Temperature and humidity data were taken from routine measurements of micro-meteorological parameters at our site and were averaged over the respective sampling periods.

It is common practice to present mixing ratios of atmospheric trace gases, however, particulate matter is often given in mass per volume concentration. In this work, we compare mixing ratios of both gaseous and

particulate compounds for the sake of direct inter-comparability of molar units in both phases. Mixing ratios ξ of particulate matter may be calculated from mass concentration c using the ideal gas law through

$$\xi = \frac{c}{M} \frac{RT}{p}$$

with c , the mass concentration of the particulate substance in $\mu\text{g m}^{-3}$, M , the molar mass of the particulate substance in g mol^{-1} , R , the universal gas constant $8.3 \text{ J mol}^{-1} \text{ K}^{-1}$, T , the ambient temperature in K, and p , the air pressure in kPa, yielding the molar fraction in nmol mol^{-1} (or ppbv). We used a constant value of 24.4 l mol^{-1} for the ideal gas law term, representing the standard temperature (25°C) and pressure (101.3 kPa) conditions.

3. Results and discussion

A wide variety of air masses differing in chemical composition arrive at our ecosystem research site, depending on various factors such as season, time of day, regional emissions, and meteorological conditions. The following section is intended to give an overview of these variations, presenting data of particulate and gaseous nitrogen compounds.

Table 2 displays typical mixing ratios of particulate nitrate, ammonium and sulfate as well as characteristic mixing ratios of ammonia during the measuring period from 1998 through 2000. The given range of HNO_3 mixing ratios was obtained during the mentioned two intensive periods in 2000.

The wide range of mixing ratios indicates large variations in the chemical composition of air masses arriving at the “Waldstein” site. However, taking a closer look at the particulate compounds, we find typical patterns of the chemical composition of aerosol particles depending on particle size. In Fig. 2, we present the median mixing ratio composition of aerosol particles in

Table 2

Range of mixing ratios of the three main inorganic ions NO_3^- , NH_4^+ , and SO_4^{2-} as well as gaseous HNO_3 and NH_3 in the “Fichtelgebirge” mountains. Displayed are median mixing ratios and the minimum and maximum mixing ratios for all species

	Median (ppbv)	Minimum (ppbv)	Maximum (ppbv)
NH_4^+	1.70	0.25	6.34
NH_3	0.36	0	2.79
NO_3^-	0.62	0.02	2.02
HNO_3	0.15	0.05	0.71
SO_4^{2-}	0.45	0.11	2.96

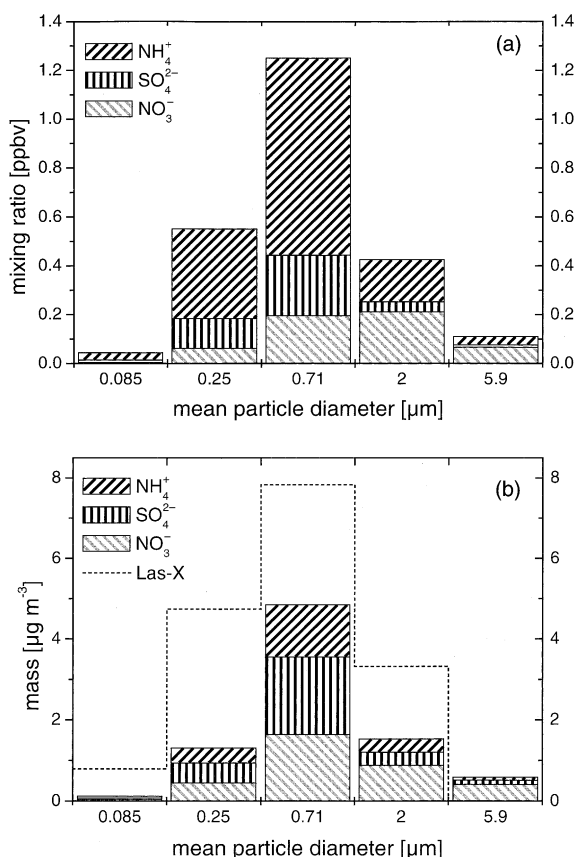


Fig. 2. (a) Median mixing ratios of ammonium, nitrate and sulfate in five particle size ranges as obtained by 86 impactor measurements. (b) Particle mass distribution of ammonium, nitrate and sulfate and total mass distribution calculated from particle number distributions measured with a LAS-X particle spectrometer, both for February 4, 2000. For the largest particles, no total particle mass (LAS-X) was calculated due to experimental limitations.

five size ranges (Fig. 2a), and the mass distribution of ammonium, nitrate and sulfate (Fig. 2b) as determined on a specific day.

Obviously, the highest abundance of particulate compounds resides within a size range with a mean particle diameter of 0.71 μm. This leads to the conclusion that we collected the atmospheric ammonium, nitrate and sulfate almost completely. The distribution mode corresponds very well with the theoretically expected accumulation mode in the range from 0.1 to 1.0 μm particle diameter. Looking at the median distribution in more detail, we can observe distinctive chemical compositions in fine and coarse atmospheric particles, respectively. In small particles, the ammonium ion dominates, contributing more than 65% of the molar concentration. However, with increasing particle size, the ammonium fraction decreases sharply. In contrast,

the nitrate fraction rises with increasing particle size from less than 10% to more than 50% over the studied size range, thus dominating the large particles. This dominance might be explained by condensation of HNO₃ on large sea salt particles, found principally in the coarse mode. H₂SO₄ can react with sea salt as well to form sodium sulfate. However, this reaction selectively takes place on smaller particles. Ten Brink (1998) assumes that this discrepancy might be explained by distinct kinetics of these two reactions, respectively. The sulfate fraction remains small over all size ranges, decreasing from about 20% in the smallest particles to less than 10% in the largest ones. This relatively small fraction of sulfate ions contrasts previous results for the “Fichtelgebirge” mountains. Eiden et al. (1989) and Peters and Bruckner-Schatt (1995) found sulfate to be the most important inorganic ion in the atmospheric aerosol in this area. However, emissions of SO₂ leading to particulate sulfate have decreased dramatically over the last 15 years in most parts of Europe, whereas a decrease in atmospheric nitrogen concentrations could not be observed (Klemm and Lange, 1999). It is important to point out once again that only ammonium, nitrate and sulfate were investigated in this study. These inorganic ions dominate the total particulate mass in the size range of the accumulation mode, whereas for smaller and larger particles, additional compounds might become relevant. In Fig. 2b, a comparison of the mass distribution of these three inorganic ions and the mass distribution as calculated from particle size distributions is shown for February 4, 2000, as an example. Assuming spherical particles and a particle density of 1.3 g cm⁻³, the particle mass distribution was calculated from particle number measurements using a laser particle spectrometer (LAS-X, PMS). Apparently, the mass distribution of ammonium, nitrate and sulfate always stays below the calculated mass distribution, which takes into account additional particle compounds. The relative deviations are large for fine particles (<0.25 μm), where organic compounds may contribute considerably to the aerosol mass. In the accumulation range, however, the three investigated inorganic ions constitute more than 60% of the particle mass. For coarse particles again, we expect large deviations accounting for additional compounds such as Ca²⁺, Mg²⁺, and K⁺ (Ansari and Pandis, 2000), yet no particle mass was calculated from size distributions for the largest particles due to experimental limitations.

In Fig. 3, median concentrations of both the gaseous and particulate species of reduced and oxidized nitrogen are displayed for measurements conducted in February 2000 (top panel) and in May 2000 (bottom panel).

These pie charts represent typical compositions of the atmospheric nitrogen budget during wintertime and summertime, respectively. The first obvious finding is the much lower concentration of total reactive nitrogen

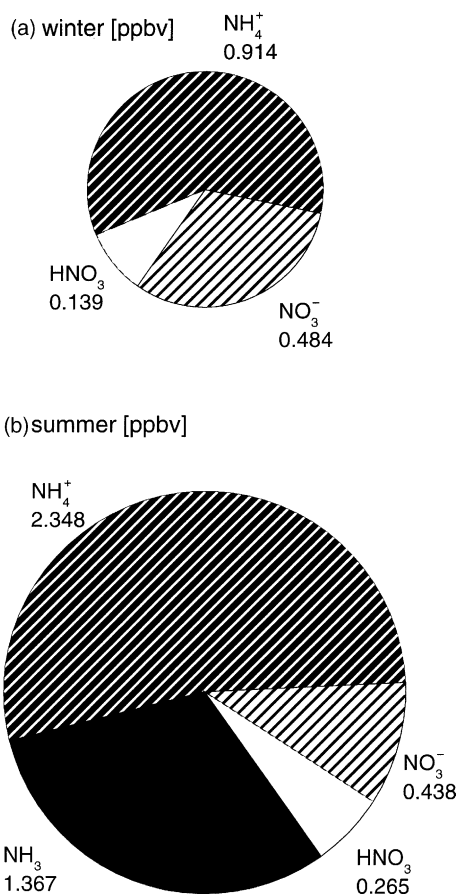


Fig. 3. Median mixing ratios of oxidized and reduced nitrogen species during winter (top) and summer (bottom) in ppbv. The circle areas are representative of the total mixing ratios. Note: NH_3 median mixing ratio was below detection limit in wintertime.

(excluding NO_x) during winter. The median mixing ratios of NH_3 , NH_4^+ , HNO_3 , and NO_3^- total 1.54 ppbv in wintertime as compared to 4.42 ppbv during summer. While gaseous ammonia is not relevant during winter (note that the median mixing ratio of NH_3 is below the detection limit for the measuring period in February), particulate ammonium dominates the distribution during both periods. Particulate nitrate mixing ratios remain constant throughout the measurements, thus contributing a much larger relative fraction of particulate oxidized nitrogen in wintertime. The particulate species dominate the gaseous compounds with an overall fraction of more than 90% in winter and still more than 60% in summer. This is due to the high water solubility and reactivity of gaseous NH_3 (Clegg and Brimblecombe, 1989) and HNO_3 (Schwartz and White, 1981; Lelieveld and Crutzen, 1991). The gaseous compounds are very effectively incorporated into deliquescent particles or droplets, thereby forming the particulate spe-

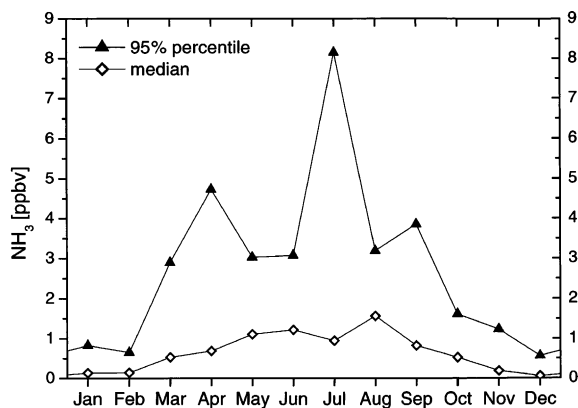


Fig. 4. Seasonal pattern of ammonia mixing ratios (in ppbv) at our site. Diamonds represent monthly median mixing ratios, triangles represent monthly 95% percentiles. Both curves were obtained from 1 h-averages of NH_3 from the years 1998 through 2000.

cies. Thus, we can expect particulate phases to dominate even at low relative humidities. However, our measurements also reflect the increasing importance of the gaseous species during summertime. For example, nitric acid mixing ratios are roughly double in summer as compared to those in winter. Ammonia contributes more than 30% of the investigated nitrogen species in summertime, while in exactly 50% of the wintertime measurements, NH_3 is not observed at all. The variability of NH_3 is reflected in a strong seasonal emission pattern of ammonia as shown in Fig. 4.

Displayed are monthly median mixing ratios of NH_3 (diamonds) and monthly 95% percentiles (triangles) obtained from hourly averages of 1998 through 2000. In summertime, large amounts of ammonia are emitted from agricultural activity, whereas during winter (November 15–January 15), no liquid manure spreading is allowed. This is consistent with high NH_3 mixing ratios in summer and low NH_3 mixing ratios in winter. Overall, the site is clearly dominated by reduced nitrogen species (NH_4^+ and NH_3) constituting roughly 60% of the total investigated nitrogen compounds in winter and almost 85% in summer. These figures indicate the prevailing influence of agricultural emissions as compared to photochemical oxidation processes at our site.

As we have found in the previous section, there is a substantial difference in the distribution of reduced and oxidized nitrogen between the particulate and gas phases during summer and winter. Therefore, it might be interesting to take a closer look at the phase partitioning of $\text{NH}_3/\text{NH}_4^+$ and $\text{HNO}_3/\text{NO}_3^-$ with respect to ambient temperature and humidity conditions, as displayed in Fig. 5.

The fraction of material present in the gas phase is shown on a molecular basis for reduced (circles) and

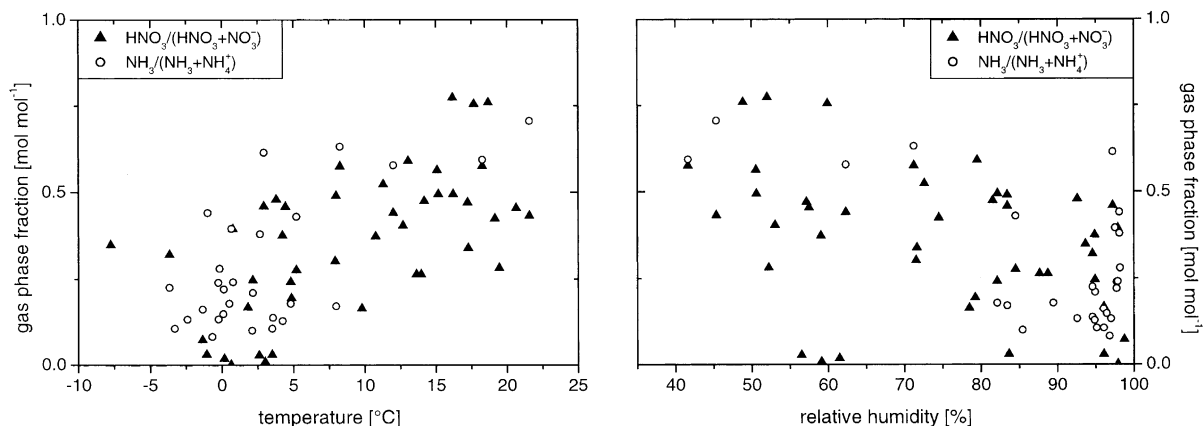


Fig. 5. Gas phase fraction of reduced (circles) and oxidized (triangles) nitrogen versus temperature (left) and relative humidity (right).

oxidized (triangles) nitrogen. Both the $\text{NH}_3/(\text{NH}_3 + \text{NH}_4^+)$ ratio and the $\text{HNO}_3/(\text{HNO}_3 + \text{NO}_3^-)$ ratio exhibit a dependence on temperature and relative humidity. The gas phase fraction increases with increasing temperature (Fig. 5, left panel), and decreases with increasing relative humidity (Fig. 5, right panel). Hence, the importance of the gas phases increases with increasing temperature and decreasing relative humidity. Overall, we observe a strong dependence of the phase partitioning of reduced and oxidized nitrogen on temperature and humidity conditions, even though the chemical composition of the investigated air masses was highly variable.

Taking into account the rural setting of our site, we expect that arriving air masses have already undergone significant transformation processes during transport. Using the same kind of reasoning, ambient aerosol particles should be in a state of equilibrium with the surrounding gas phase. This assumption is supported by the fact that the measured aerosol size distributions exhibit maxima in the accumulation size range (Fig. 2). In order to further verify this hypothesis, we calculated the theoretical thermodynamic equilibrium of reduced ($\text{NH}_3/\text{NH}_4^+$) and oxidized ($\text{HNO}_3/\text{NO}_3^-$) nitrogen species between the particulate and gas phases and compared the model results with our measurements. The prediction of gas–particle partitioning of volatile inorganic species on the basis of thermodynamic relations has been investigated for more than 20 years now (Stelson et al., 1979). Since then, a variety of thermodynamic equilibrium models have been developed. In most cases, different equilibrium models, such as SEQUILIB (Pilinis and Seinfeld, 1987), SCAPE/SCAPE2 (Kim et al., 1993a,b; Kim and Seinfeld, 1995), MARS-A (Binkowski and Shankar, 1995), AIM2 (Clegg et al., 1998), and EQUISOLV II (Jacobson, 1999) yield comparable results for the partitioning of oxidized and reduced nitrogen (Zhang et al., 2000). We applied the Aerosol

Inorganics Model 2 (AIM2) assuming internal mixing of aerosol particles, as interactions between the particulate and gas phase are not evaluated on the single particle level in the model. Even though we found strong indications of predominantly external mixing of the atmospheric aerosol at our site (Held et al., 2002), we compare model results to our original measurements in the following paragraph.

Fig. 6 shows gas phase concentrations of NH_3 and HNO_3 as determined by denuder measurements and by thermodynamic model calculations, respectively. In both cases, there is very good agreement between measurement and model results. Mixing ratios of NH_3 (left panel) were usually very low during the measuring period in February 2000. From February 6 to 8, however, elevated levels of NH_3 could be observed reaching a maximum of 0.7 ppbv. For this period, the model underestimates the NH_3 mixing ratio to a small degree, whereas during low NH_3 level conditions, the model expects some more NH_3 to be in the atmospheric gas phase. The pattern of HNO_3 (right panel) is more variable as compared to NH_3 , but still, the model curve imitates the measurements very well. For the first three measurements, the model slightly underestimates the HNO_3 mixing ratio, whereas all other measurements are overestimated by the model, especially between February 10 and 12. In previous studies, several authors found good agreement between theoretical calculations and their measurements (Doyle et al., 1979; Harrison and Pio, 1983; Hildemann et al., 1984; Chang et al., 1986; Lewin et al., 1986), especially under low relative humidities and high temperatures (Grosjean, 1982; Allen et al., 1989). For relative humidities above 80% and temperatures below 0 °C (like those measured during the investigated period in February 2000), some authors found higher measured concentrations as compared to their model results (Erisman et al., 1988; Allen et al., 1989). Our results correspond very well with these findings. To assess the combined influence of temperature

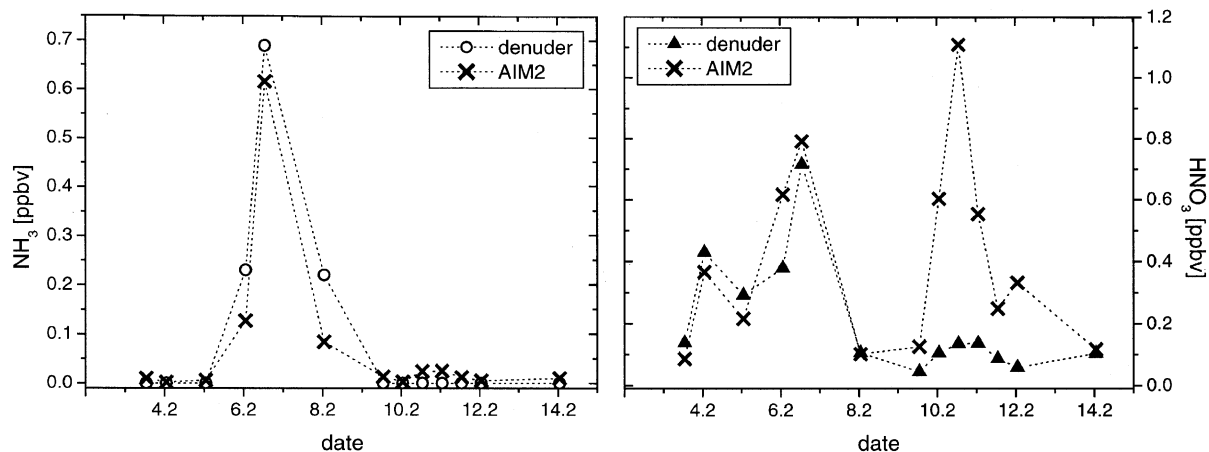


Fig. 6. Comparison of NH_3 (left) and HNO_3 (right) mixing ratios (in ppbv) as determined by denuder measurements and by model calculations using the Aerosol Inorganics Model 2 (AIM2, Clegg et al., 1998).

and relative humidity on the equilibrium between the gaseous and particulate compounds, we calculate the phase partitioning of reduced nitrogen in thermodynamic equilibrium for varying temperature and relative humidity starting with the median chemical composition from all measurements. The temperature is varied between -5 and 30 $^{\circ}\text{C}$, and relative humidity between 40% and 100%.

The three-dimensional surface in Fig. 7 represents the specific $\text{NH}_3/\text{NH}_4^+$ ratio for an established thermodynamic equilibrium at any given temperature and relative humidity. The plane surface at high temperatures and

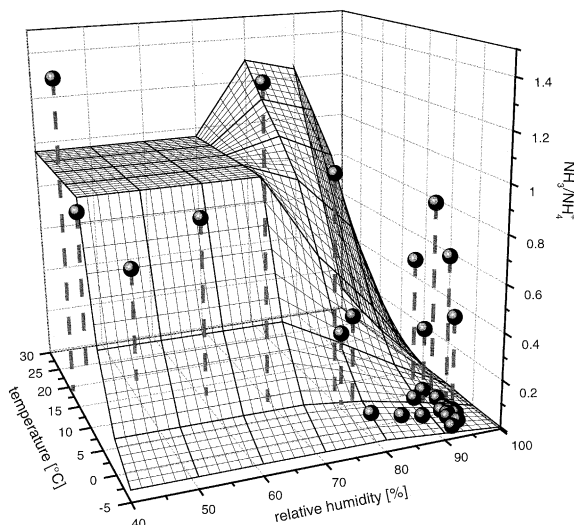


Fig. 7. Three-dimensional representation of the gas/particle ratio of reduced nitrogen in a state of thermodynamic equilibrium for varying temperature and relative humidity (AIM2 model calculation). The spheres represent the $\text{NH}_3/\text{NH}_4^+$ ratios as measured at the “Waldstein” site.

low relative humidities indicates the presence of solid ammonium sulfate. In addition to ammonium sulfate, we can expect solid $(\text{NH}_4\text{NO}_3)_2 \cdot (\text{NH}_4)_2\text{SO}_4$ to occur at temperatures below 5 $^{\circ}\text{C}$. Through evaporation of volatile ammonium nitrate, the NH_3 mixing ratio is elevated with increasing temperature, thus also increasing the $\text{NH}_3/\text{NH}_4^+$ ratio. At 5 $^{\circ}\text{C}$, ammonium nitrate is completely evaporated. Since ammonium sulfate is not volatile, any further increase in temperature does not affect the mixing ratio of NH_3 . Therefore, ammonia and ammonium incorporated in non-volatile ammonium sulfate exhibit a constant gas/particle ratio represented by the plane surface. At relative humidities exceeding 70%, ammonium sulfate spontaneously absorbs water, producing a saturated aqueous solution. Solid phases cease to exist above this so-called deliquescence relative humidity. The spheres in Fig. 7 represent the $\text{NH}_3/\text{NH}_4^+$ ratio as measured at our site. Apparently, our measurements match the theoretical surface quite well. Some outliers at high relative humidities and low temperatures may be explained by low absolute NH_3 mixing ratios, which inevitably reduces the accuracy of the measurement. At these concentrations, even slightly inaccurate measurements of NH_3 lead to rather large errors in the gas/particle ratio. However, we conclude from the good agreement between theoretical calculations and our measurements that thermodynamic equilibrium models are applicable at our site and useful for obtaining deeper insight into the phase partitioning of oxidized and reduced nitrogen species.

4. Conclusions

We present ambient mixing ratios of ammonia, ammonium, nitric acid, and nitrate under various meteo-

rological conditions. However, for a reliable estimation of the atmospheric nitrogen input through gaseous and particulate compounds, we need to combine the information about the concentration of these substances with their respective deposition velocities. For deposition of particulate compounds, particle size is the critical factor. Our results endorse the establishment of an accumulation mode in the size range between 0.1 and 1 μm particle diameter. In this size range, particle deposition velocities exhibit a minimum, and increase for smaller as well as larger particles. In the next few years, the application of eddy correlation techniques for the determination of vertical particle fluxes promises to deepen our knowledge about particulate nitrogen deposition. However, the estimation of atmospheric NH_3 fluxes remains highly complicated, in spite of the vast amount of research focussing on vegetation-atmosphere interaction with regard to NH_3 . Furthermore, the concept of a NH_3 compensation point governing the deposition or emission of ammonia imposes great difficulties on a comprehensive approach to determine ammonia fluxes between vegetation or soil surface and the atmosphere. Yet the results in this study demonstrate the predominance of reduced nitrogen species at a rural, forested site, making an accurate estimate of reduced nitrogen deposition even more important. The dependence of the gas/particle ratio of both oxidized and reduced nitrogen on temperature and relative humidity together with the good agreement between thermodynamic equilibrium model results and our measurements encourages further application of this model to obtain deeper insight into the gas/particle partitioning of oxidized and reduced nitrogen. Combining these results with further research on deposition mechanisms of gaseous and particulate species thus enhances our ability to estimate gaseous and particulate input of atmospheric nitrogen into terrestrial ecosystems.

Acknowledgements

This work was funded by the Bundesministerium für Bildung und Forschung (BMBF) through grant No. PT BEO 51–0339476 C. We appreciate the help and support of the Zentrale Analytik of the Bayreuth Institute for Terrestrial Ecosystem Research with chemical analysis. Further, we are indebted to S. Clegg and A. Wexler for providing the AIM model for general use in the world wide web, and to T. Ferdelman for language-editing of the manuscript.

References

Allen, A.G., Harrison, R.M., Erisman, J.W., 1989. Field measurements of the dissociation of ammonium nitrate

- and ammonium chloride aerosols. *Atmos. Environ.* 23, 1591–1599.
- Ansari, A.S., Pandis, S.N., 2000. The effect of metastable equilibrium states on the partitioning of nitrate between the gas and aerosol phases. *Atmos. Environ.* 34, 157–168.
- Binkowski, F.S., Shankar, U., 1995. The regional particulate matter model, I: model description and preliminary results. *J. Geophys. Res.* 100, 26191–26209.
- Chang, Y.S., Carmichael, G.R., Kurita, H., Ueda, H., 1986. An investigation of the formation of ambient NH_4NO_3 aerosol. *Atmos. Environ.* 20, 1969–1977.
- Clegg, S.L., Brimblecombe, P., 1989. Solubility of ammonia in pure aqueous and multicomponent solutions. *J. Phys. Chem.* 93, 7237–7238.
- Clegg, S.L., Brimblecombe, P., Wexler, A.S., 1998. Thermodynamic model of the system $\text{H}^+ - \text{NH}_4^+ - \text{SO}_4^{2-} - \text{NO}_3^- - \text{H}_2\text{O}$ at tropospheric temperatures. *J. Phys. Chem. A* 102, 2137–2154. Available from <<http://www.hpcl.uea.ac.uk/~e770/aim.html>>.
- Doyle, G.J., Tuazon, E.C., Graham, R.A., Mischke, T.M., Winer, A.M., Pitts, J.N., 1979. Simultaneous concentrations of ammonia and nitric acid in a polluted atmosphere and their equilibrium relationship to particulate ammonium nitrate. *Environ. Sci. Technol.* 13, 1416–1419.
- Eiden, R., Förster, J., Peters, K., Trautner, F., Herterich, R., Gietl, G., 1989. Air pollution and deposition. In: Schulze, E.D., Lange, O.L., Oren, R. (Eds.), *Forest decline and air pollution*. Springer, Berlin, pp. 57–103.
- Erisman, J.W., Vermetten, A.W.M., Asman, W.A.H., Waijers-Ijpelaar, A., Slanina, J., 1988. Vertical distribution of gases and aerosols: the behaviour of ammonia and related components in the lower troposphere. *Atmos. Environ.* 22, 1153–1160.
- Friedlander, S., 2000. *Smoke, dust, and haze: Fundamentals of aerosol dynamics*. Oxford University Press, New York.
- Grosjean, D., 1982. The stability of particulate nitrate in the Los Angeles atmosphere. *Sci. Total Environ.* 25, 263–275.
- Harrison, R.M., Pio, C.A., 1983. An investigation of the atmospheric $\text{HNO}_3 - \text{NH}_3 - \text{NH}_4\text{NO}_3$ equilibrium relationship in a cool humid climate. *Tellus* 35B, 155–159.
- Held, A., Hinz, K.-P., Trimborn, A., Spengler, B., Klemm, O., 2002. Chemical classes of atmospheric aerosol particles at a rural site in central Europe during winter. *J. Aerosol Sci.* 33, 581–594.
- Hildemann, L.M., Russell, A.G., Cass, G.R., 1984. Ammonia and nitric acid concentrations in equilibrium with atmospheric aerosols: experiment vs theory. *Atmos. Environ.* 18, 1737–1750.
- Jacobson, M.Z., 1999. Studying the effects of calcium and magnesium on size-distributed nitrate and ammonium with EQUISOLV II. *Atmos. Environ.* 33, 3635–3649.
- Keuken, M.P., Schoonebeek, C.A.M., van Wensveen-Louter, A., Slanina, J., 1988. Simultaneous sampling of NH_3 , HNO_3 , HCl , SO_2 and H_2O_2 in ambient air by a wet annular denuder system. *Atmos. Environ.* 22, 2541–2548.
- Kim, Y.P., Seinfeld, J.H., Saxena, P., 1993a. Atmospheric gas aerosol equilibrium, I: Thermodynamic model. *Aerosol Sci. Technol.* 19, 157–181.
- Kim, Y.P., Seinfeld, J.H., Saxena, P., 1993b. Atmospheric gas aerosol equilibrium, II: Analysis of common approximations

- and activity coefficient calculation methods. *Aerosol Sci. Technol.* 19, 182–198.
- Kim, Y.P., Seinfeld, J.H., 1995. Atmospheric gas–aerosol equilibrium III: Thermodynamics of crustal elements Ca^{2+} , K^+ , and Mg^{2+} . *Aerosol Sci. Technol.* 22, 93–110.
- Klemm, O., Lange, H., 1999. Trends of air pollution in the Fichtelgebirge mountains, Bavaria. *Environ. Sci. Pollut. R.* 6, 193–199.
- Lelieveld, J., Crutzen, P.J., 1991. The role of clouds in tropospheric photochemistry. *J. Atmos. Chem.* 12, 229–267.
- Lewin, E.E., de Pena, R.G., Shimshock, J.P., 1986. Atmospheric gas and particle measurements at a rural northeastern US site. *Atmos. Environ.* 20, 59–70.
- Ludwig, J., Klemm, O., 1990. Acidity of size-fractionated aerosol particles. *Water Air Soil Pollut.* 49, 35–50.
- Matzner, E., Alewell, C., Bittersohl, J., Lischeid, G., Kammerer, G., Manderscheid, B., Matschonat, G., Moritz, K., Tenhunen, J.D., Totsche, K., 2001. Biogeochemistry of a spruce forest catchment of the Fichtelgebirge in response to changing atmospheric deposition. In: Tenhunen, J.D., Lenz, R., Hantschel, R. (Eds.), *Ecosystem approaches to landscape management in Central Europe*. Ecological Studies, vol. 147, Springer, Berlin, pp. 463–503.
- Peters, K., Bruckner-Schatt, G., 1995. The atmospheric input of inorganic nitrogen and sulphur by dry deposition of aerosol particles to a spruce stand. In: Heij, G.J., Erisman, J.W. (Eds.), *Acid rain research: Do we have enough answers?* Elsevier Science, Amsterdam, pp. 149–160.
- Pilinis, C., Seinfeld, J.H., 1987. Continued development of a general equilibrium model for inorganic multicomponent atmospheric aerosols. *Atmos. Environ.* 21, 2453–2466.
- Schulze, E.D., Lange, O.L., Oren, R. (Eds.), 1989. *Forest decline and air pollution*. Ecological Studies, vol. 77, Springer, Berlin.
- Schwartz, S.E., White, W.H., 1981. Solubility equilibria of the nitrogen oxides and oxyacids in dilute aqueous solution. In: Pfafflin, J.R., Ziegler, E.N. (Eds.), *Advances in Environmental Science and Engineering*. Gordon and Breach Science Publishers, New York, pp. 1–45.
- Seinfeld, J.H., Pandis, S.N., 1998. *Atmospheric chemistry and physics: from air pollution to climate change*. John Wiley & Sons, New York.
- Stelson, A.W., Friedlander, S.K., Seinfeld, J.H., 1979. A note on the equilibrium relationship between ammonia and nitric acid and particulate ammonium nitrate. *Atmos. Environ.* 13, 369–371.
- Sutton, M.A., Schjorring, J.K., Wyers, G.P., 1995. Plant–atmosphere exchange of ammonia. *Phil. Trans. R. Soc. London A* 351, 261–278.
- Ten Brink, H.M., 1998. Reactive uptake of HNO_3 and H_2SO_4 in sea-salt (NaCl) particles. *J. Aerosol Sci.* 29, 57–64.
- Wrzesinsky, T., Klemm, O., 2000. Summertime fog chemistry at a mountainous site in central Europe. *Atmos. Environ.* 34, 1487–1496.
- Wyers, G.P., Otjes, R.P., Slanina, J., 1993. A continuous-flow denuder for the measurement of ambient concentrations and surface-exchange fluxes of ammonia. *Atmos. Environ.* 27A, 2085–2090.
- Zhang, Y., Seigneur, C., Seinfeld, J.H., Jacobson, M., Clegg, S.L., Binkowski, F.S., 2000. A comparative review of inorganic aerosol thermodynamic equilibrium modules: similarities, differences, and their likely causes. *Atmos. Environ.* 34, 117–137.